Accurate vapor pressure measurements of supercooled water in the temperature range between 252 K and 273 K

ACCURATE VAPOUR PRESSURE MEASUREMENTS OF SUPERCOOLED WATER IN THE TEMPERATURE RANGE BETWEEN 252 K AND 273 K

Authors: G. Beltramino, L. Rosso, R. Cuccaro, S. Tabandeh, D. Smorgon, V. Fernicola

Affiliation: INRIM - Istituto Nazionale di Ricerca Metrologica, Torino, Italy

Corresponding author: L. Rosso (*l.rosso@inrim.it*)

Abstract

The accurate knowledge of the saturation vapour pressure of liquid water and ice has a great importance in a host of applications where humidity measurements are involved since it enables the correct conversion among different physical quantities that quantify the water vapour amount of a humid gas mixture.
More specifically, accurate saturation vapour pressure measurements of supercooled water are strongly required in meteorology and atmospheric sciences, especially in cloud microphysics studies.
Considering the importance of this kind of measurements and the limited availability of experimental data in the literature, further measurements in the metastable region were carried out at the Istituto Nazionale di Ricerca Metrologica (INRIM).
The sample cell used in the experiment is a U-shaped capillary tube made of borosilicate glass, whose temperature is kept constant by immersion in a thermostatic bath with a high temperature stability (about 1 mK). The cell is connected to a capacitive diaphragm pressure gauge measuring the equilibrium water vapour pressure, that varies between about 116 Pa at $T = 252.25$ K and 615 Pa at $T = 273.25$ K.
In the present work, the measuring method and the experimental setup are described and the measurements results reported. The results obtained in the whole temperature range are compared with those available in the literature and with the commonly adopted saturation vapour pressure formulations. A complete uncertainty budget is also given, resulting in an expanded relative uncertainty ranging from 0.06 % at 273.25 K to 0.20 % at 252.25 K.

Keywords: supercooled water; saturation vapour pressure; capillary tube; water vapour properties.

1. Introduction

A precise knowledge of the saturation vapour pressure as a function of the temperature in the supercooled water region is extremely important in cloud microphysics [1], in order to properly calculate the nucleation and growth of water and ice droplets in the atmosphere as well as their latent heat, key parameters in weather modelling and forecasting.
Several equations [2-11] describe the saturation water vapour pressure versus the temperature. Some of them are empirical, but most of them are based on the well-known Clausius-Clapeyron equation:

$$\frac{dp}{dT} = \frac{L_{\mathrm{liq}} p}{RT^2}, \tag{1}$$

in which the water vapour is approximated as an ideal gas, R is the molar gas constant, p the saturation vapour pressure, L_{liq} the latent heat of evaporation and T is the thermodynamic temperature.
Recently, an equation of state in the form of the Gibbs energy function for the thermodynamic properties of supercooled water has been provided by Holten et al. [12, 13]. The equation is valid from the homogeneous ice nucleation temperature to 300 K, at pressures up to 400 MPa. The equation is based on the so-called two-state model, which assumes liquid water as a mixture of two distinct local structures (high-density and low-density). Their competition explains the thermodynamic anomalies observed in cold water at a temperature of about 228 K at atmospheric pressure [14].
For temperatures below 273.15 K, the lack of experimental data, due to the difficulties in carrying out measurements in the metastable state, yields diverging extrapolated values of saturation water vapour pressure, especially at low temperatures.
Among the few experimental data present in the literature, notable are those of saturation vapour pressure over supercooled liquid water obtained by Scheel and Heuse [15] at the beginning of the 20$^{\mathrm{th}}$ century, as well as those from Bottomley in 1978 [16] and from Kraus and Greer in 1984 [17]. The latter were able to measure saturation vapour pressure at temperatures down to 254 K. Even wider was the temperature range explored by Fukuta and Gramada in 2003 [18], from the melting point down to 243 K, by using a dew-point hygrometer method.
Recently, Beltramino et al. [19] was able to carry out accurate saturation vapour pressure measurements down to 261 K, maintaining water in supercooled state by adopting a degassing procedure based on several cycles of water freezing, high-vacuum pumping and thawing under low pressure.
Keeping water in a supercooled state becomes increasingly demanding as the temperature decreases from the melting point, especially for the long time intervals (several hours) usually required for accurate measurements. Mossop [20], by using capillary tubes with internal diameters between 0.2 mm and 0.3 mm, internally coated with a hydrophobic layer, was able to keep water in a liquid state down to about 238.15 K, not so far from the homogenous nucleation temperature. The hydrophobic coating prevented the formation of a thin film of water on the walls of cleaned glass tubes, thus mitigating the risk of freezing.

At a pressure of about 0.1 MPa the temperature limit for homogeneous nucleation of water, which coincides with the lowest attainable temperature in the supercooled state, is about 232 K. Its value decreases with increasing pressure, reaching a minimum of about 181 K at a pressure of 200 MPa, with a slight change when the pressure further increases up to 300 MPa [21]. On the other hand, it has been shown experimentally that a "glassy" form of water, also called low-density amorphous (LDA) ice, can exist when micrometre-sized droplets of liquid water are rapidly cooled below the glass transition temperature, i.e. about 130 K at atmospheric pressure [22]. Between the homogeneous nucleation temperature and the glass transition temperature, a "no man's land" exists, where it is not experimentally possible to attain a metastable liquid water state due to its high crystallization rate.

Recently, evidence has been found of a new low-temperature limit for supercooling of about 225 K, both by simulation [23, 24] and by experiments [25]. This state is limited to nanoscopic volumes of water (droplets with diameters of some micrometres confined in micropores) lasting at most some milliseconds.

New measurements of the saturation vapour pressure over supercooled liquid water along the saturation line have been carried out at INRIM in the temperature range between 252 K and 273 K. The aim of the work was to investigate a range where few data were previously reported [15-19, 26]. Although results of notable experiments, saturation vapour pressure values reported in literature are often lacking of a clear uncertainty assessment and few information about their traceability can be deduced. In this work, both experimental data and associated uncertainties are pointed out, providing an accurate evaluation of the measurement uncertainty. Moreover details on the instruments calibration against INRIM reference standards are explicitly mentioned. The significance of the comparison with literature data [15-19, 26] and known formulations [2-13] is also commented.

2. Measurement method and experimental apparatus

In the present work, a static pressure measurement is used to determine the saturation vapour pressure in the temperature range of interest.

The experimental apparatus, depicted in Figure 1, consists essentially of a custom sample cell, a triple point of water (TPW) cell, a differential pressure gauge and a suitable valve manifold for the connection of both cells to the pressure gauge and to a turbo-molecular vacuum pump (TMP).

The sample cell consists of a U-shaped, borosilicate-glass capillary tube, about 250 mm long with a 6 mm outer diameter and a 0.4 mm inner diameter. The cell shape was chosen because both opened ends allow an easier filling and degassing. The use of a capillary tube with an inner diameter of 0.5 mm or less was deemed necessary to keep water in supercooled state at very low temperatures (253 K or even lower), as observed by Hosler and Hosler [27]. They found that the supercooling degree of their water samples was independent of the length, volume and surface area of the samples, depending only upon the diameter of the containing tube; however, Mossop [20] discovered that the volume independence holds only for non-hydrophobic tubes, which is the case of the capillary tube used in this work. According to them, the importance of the diameter of the tube lies in the fact that the formation of an electrical double layer at the surface of a water drop makes spontaneous nucleation more difficult, due to a slight change in the normal atomic structure of water; so, the only geometrical parameter that

determines the supercooling degree seems to be the maximum distance between any point in the liquid and the nearest surface.

An important preliminary step in the arrangement of the experiment is the filling of the capillary tube with water; it should be performed in such a way to reduce the entrance of ambient air in the sample cell. In fact, as observed by Mossop [20], the particulate matter contained in ambient air settles on the free-water internal wall of the sample cell, causing the formation of ice around it during the water vapour sublimation, when approaching the equilibrium with respect to liquid water. The presence of these freezing nuclei limits downwards the temperature at which water remains in the liquid phase, prompting the transition from the liquid to the solid phase. For this reason, a dedicated filling procedure was adopted in this experiment to reduce the entrance of ambient air into the sample cell and limit (but not eliminate) the settlement of the freezing nuclei. This procedure may be summarized as follows. The cylindrical cell used for the realization of the triple point of water (TPW) was filled with about 60 ml of distilled water, with a purity level corresponding to an electrical conductance lower than 0.7 $\mu S\ cm^{-1}$; then, the TPW cell was connected with the capillary tube, thus leaving the liquid water to evaporate at room temperature and fill the volume inside the capillary tube. Subsequently, the latter was partially immersed in a thermostatic bath, kept at a temperature of 263 K, in order to condensate the water vapour on the wall of the immersed section. The final result was a column of liquid water a few centimetres high lying at the bottom of the U-shaped tube cell.

Once filled with distilled water, the sample cell and the TPW cell were fully immersed into the thermostatic liquid bath. The temperature of the sample cell was measured by means of a 100-Ω platinum resistance thermometer (PRT) inserted into a thermowell inside the TPW cell. The PRT, calibrated at fixed points and traceable to ITS-90, was placed at a depth such that the sensing element was aligned with the water-air interface inside the capillary sample cell. The temperature stability of the thermostatic bath was better than 1 mK at 243.15 K when ethanol was used as the working fluid.

To successfully maintain the water at the supercooled liquid state down to 252.25 K for a period long enough to obtain precise and reliable saturation vapour pressure measurements, the water sample was subjected to a further degassing process. It consists of several cycles of water freezing, pumping by means of a turbo-molecular pump, and thawing under low pressure conditions. More than ten cycles were carried out until no air bubbles were trapped inside the water. The removal of air bubbles is facilitated by the U-shape of the capillary tube, which enables to vacuum pump to operate simultaneously on both the sides of the water column. At the end of the procedure, the height of the water column inside the capillary tube was usually less than 100 mm, corresponding to about 0.1 ml of water.

Before any saturation vapour pressure measurement, to ensure that no other volatile components except for water vapour were present in the system volume, the sample cell was isolated from the pressure gauge and the system was carefully evacuated. Then, the sample cell was immersed in the thermostatic bath and the connection via the manifold was re-established. Finally, the measurement of the pressure was carried out when a water liquid-vapour equilibrium is achieved.

Four saturation vapour pressure measurement runs were performed. Three runs were carried out in the range from 255.15 K to 273.15 K, and the fourth between 253.15 K and 273.15 K.

For each run the pressure was measured at temperature steps of 1 K, starting from the lowest temperature. To perform the measurement of saturation vapour pressure below 255.15 K, the height of the water column inside the capillary was reduced to few millimetres, with a volume of the liquid comparable to that of a small droplet (ca. 5µl). Between each run the sample cell was isolated from the pressure gauge and the system evacuated in order to check for any zero drift of the manometer and zeroed when needed.

Within each run, the equilibrium vapour pressure was measured at each investigated temperature. It was observed that, once the temperature-pressure equilibrium was attained, the pressure reading increased at a rate of about 30-40 mPa h^{-1}. This effect might be due to small air leaks into the system through the various metal-gasket fittings and flanges. Indeed, the observed trend is consistent with the leak-proof specifications of these system components. In order to obtain accurate and consistent pressure measurements, a linear back-extrapolation of the water vapour pressure to the initial time t_0 was carried out, where t_0 is the time at which the system, except for the capillary tube, was completely evacuated and the manifold valve opened. An accurate extrapolation requires at least 2 hours of data acquisition, which is also the time required for the vapour pressure to equilibrate from vacuum. A significant time interval due to the small interfacial surface between liquid water and water vapour (~ 0.25 mm^2).

At the end of the last run, a triple point of water (TPW) experiment was realized in the cylindrical cell connected to the same manifold, thus obtaining a TPW saturation vapour pressure to be used as reference value for an *in situ* correction of the pressure gauge reading. Although a capacitive pressure gauge is in principle gas independent, as it was calibrated in pure nitrogen, but used in pure water vapour, this correction was in fact complementary to that resulting from the instrument calibration. The estimated TPW pressure extrapolated to t_0 as described above was 611.577 Pa which is close to the widely-accepted best estimate of 611.657 Pa [28].

The capacitance manometer was calibrated against the INRIM pressure reference standard. The correction factor F, i.e. calculated as the ratio between the reference pressure value p_{ref} and the measured value p_{read}, was provided at different pressures in the range from 10 Pa to 1300 Pa. A linear regression was used in order to interpolate the correction factor F in the above range; then the pressure gauge reading was multiplied by the corresponding interpolated $\hat{F}$ to obtain the corrected pressure value.

Pressure readings were also corrected for hydrostatic head and thermal transpiration effect. The hydrostatic head correction corresponds to the weight of the gas column between the liquid-vapour interface and the pressure gauge. In this work, considering that the gas column is not at a uniform temperature, and thus has not the same density all along the column, the correction was evaluated by means of the hypsometric equation. The gas column can be approximately divided in two segments, one of about 440 mm out of the bath and one of about 400 mm in the bath. The temperatures of the two segments were set to about 45 °C for the former and to the temperature of the thermostatic bath at which the measurement is performed for the latter. A stepwise temperature profile was approximated. The hypsometric equation used for the evaluation of the hydrostatic head correction is as follows:

$$p_1/\mathrm{Pa} = p_0/\mathrm{Pa} \cdot \left(e^{\frac{g}{R_V} \cdot \left(\frac{\Delta z_2}{T_{\mathrm{sample}}/\mathrm{K}} + \frac{\Delta z_1}{T_{\mathrm{man}}/\mathrm{K}} \right)} - 1 \right), \qquad (2)$$

where p_1 is the pressure at the interface liquid-vapour, p_0 is the pressure measured by the manometer, g is the local acceleration due to gravity (9.810874 m s^{-2}), R_v is the specific gas constant for water vapour (461 J kg^{-1} K^{-1}), T_{man} is the temperature of the pressure transducer (318.15 K), T_{sample} is the sample temperature, Δz_2 is the height of the gas column at T_{sample} and Δz_1 is the height of the gas column at T_{man}. The length Δz_1 and Δz_2 are equal to 440 mm and 400 mm, respectively.

The contribution of the hydrostatic head correction to the overall pressure is quite small over the whole range, adding no more than 40 mPa to the pressure reading.

The thermal transpiration effect consists in a difference between the pressure measured by the capacitance manometer and the effective pressure in the sample cell, which occurs when the pressure transducer and the cell are at different temperatures and the molecular-flow regime at low pressure comes into play.

In this work, the pressure range includes the transition between the high-pressure regime (where $p_0 = p_1$) and the molecular-flow regime, where the relationship between the sample temperature (T_{sample}), the sample pressure (p_1), the gauge temperature (T_{man}) and the gauge pressure (p_0) can be expressed by $p_0/p_1 = (T_{man}/T_{sample})^{1/2}$. The thermal transpiration effect was estimated by means of the empirical equation provided by Takaishi-Sensui [29], with coefficients taken from Yasumoto [30]. In the temperature and pressure ranges investigated, the amount of this correction is negligible as it starts to become significant at pressures lower than 100 Pa, which in this work would correspond to a sample temperature lower than 250 K.

Corrections applied to pressure measurements over the investigated temperature range are summarised in Table 1 in terms of percent values.

3. Results and Discussion

The saturation vapour pressures of supercooled water measured in the investigated temperature range 252 K to 273 K for all the four runs are reported in Table II. In the table the combined expanded uncertainty (k = 2), $U_c(p)$, is also given. The uncertainty $U_c(p)$ was estimated by combining the uncertainty contributions from temperature and pressure measurements, which are reported in details in Table III and IV, respectively. The relative expanded uncertainty of water vapour pressure varies from 0.06 % to 0.20 % with decreasing pressure.

Table III shows the uncertainty budget of the temperature measurements with the main sources of uncertainty at three different temperatures: 253 K, 263 K and 273 K, which correspond to vapour pressures of about 127 Pa, 289 Pa and 615 Pa, respectively. As Table III highlights, the largest source of uncertainty is due to the linearity of the resistance bridge. As regards the other uncertainty components, the PRT calibration contribution was estimated to be constant over the whole range as well as the thermostatic bath temperature stability and uniformity. The given estimates correspond to the worst case observed in the temperature range investigated. The combined standard uncertainty, $u_c(T)$, resulted in about 3 mK over the whole range from 252 K to 273 K.

As to pressure, Table IV shows the uncertainty budget for pressure measurements at three different pressures. The main sources of uncertainty are represented by the pressure gauge calibration and by the TPW realization which account for more than 95 % of the overall uncertainty. The zero drift of the gauge together with the span drift and linearity have also a non-negligible contribution to the uncertainty budget, as well as the thermomolecular effect

correction, while the hydrostatic head and the residual gas effect have a minor impact on the overall budget. The combined standard uncertainty, $u_c(p)$, resulted in 114 mPa and 115 mPa for saturation water vapour pressures measured at the lower and at the upper limit of the investigated range.

The experimental results of saturation vapour pressure of supercooled water are shown in Figure 2, where they are compared to the saturation vapour pressure of supercooled water as obtained by using several available formulations [2-13]. All values are presented in terms of relative pressure differences using as reference the IAPWS G12-15 formulation [13], based on the equation of state by Holten et al. [12]. The results of the present work are in agreement with the saturation vapour pressure formulations considered here, except for the Murray's Magnus equation [3]. It's worth to observe that also the agreement with the CIMO [10] and the Bolton [9] equations is limited to temperatures around the triple point of water.

In Figure 3 pressure measurements in the four runs are reported. For the sake of clarity, the uncertainty bars for the first and the fourth run are shown. Measured pressures are also compared with the measurements available in literature [15-19, 26]. All the data are plotted as differences, Δp, with respect to the IAPWS G12-15 equation. In order to make the data given by Bottomley [16] comparable with all the others, they have been re-adjusted as differences between the saturation vapour pressure of supercooled water and that of a corresponding stable ice phase at the same temperature calculated using the IAPWS 2011 formulation [31]. As Figure 3 highlights, the results of this work and measurements previously carried out by Beltramino *et al.* [19] compare favourably; they are consistent within their combined uncertainty.

Regarding measurements reported by other authors, an effective comparison is quite difficult since very few information about measurement uncertainty evaluation can be deduced by their works. For example, Kraus and Greer report an "accuracy" of their water vapour pressure data of 2.67 Pa [17], while Bottomley and Scheel and Heuse report a "reproducibility" among different runs of about 133 mPa [16] and 1.33 Pa [15] respectively. A graph in the *Corrigendum* of Cantrell's work [26] shows a measurement uncertainty of about 20 Pa, while for data given by Fukuta and Gramada no other information besides the measurement values can be found.

Furthermore in these works there is no clear evidence of the measurements traceability, as explicit references to the calibration of all instruments used to perform experiments are lacking.

4. Conclusions

An investigation of the metastable liquid-vapour equilibrium along the condensation line over a wide temperature range from the TPW down to 252 K was carried out at INRIM, using a static pressure measurement method.

The experimental apparatus used in this work consisted of a thermostatic bath, a capillary tube filled with ultra-pure water, a differential capacitive pressure gauge for vapour pressure measurements and a capsule-type PRT for the measurement of the sample temperature. The capacitance manometer and the PRT were calibrated against the INRIM pressure reference standard and at fixed points respectively to guarantee the traceability of saturation vapour pressure measurements. Potential sources of measurement uncertainty were also investigated and a clear and accurate measurement uncertainty evaluation was provided.

The obtained experimental results compared favourably with the most recent saturation vapour pressure formulations [13] and measurements [19]. On the contrary, an effective comparison with previous experiments reported in literature [15-17, 26] was hard to perform because of the lack of traceability and information about the evaluation of the measurement uncertainty.
Measurements carried out in this work further extended the experimental range investigated by [19] getting closer to the lowest temperature achieved by Kraus and Greer [17], corroborating the hypothesis about the non-reliability of their measurements below 252 K, probably due to the partial freezing of the droplets inside the measurements cell.
A further extension of the measurement range of saturation vapour pressure of supercooled water would be strongly required (e.g. down to 243 K), in order to validate the saturation vapour pressure formulations over a wider temperature range. While it would be clear the scientific impact of such an endeavour, an attempt to overcome the difficulty to reach such low temperatures could be made only by reducing the inner diameter of the capillary tube below 0.4 mm, thus further reducing the water sample size.

5. References

[1] A. Tabazadeh, Y. S. Djikaev and H. Reiss, PNAS **99**, 15873 (2002).

[2] J. A. Goff, Trans. Am. Soc. Heat. Vent., 347 (1957).

[3] F.W. Murray, J. Appl. Meteorol. **6**, 203 (1967).

[4] R.W. Hyland and A. Wexler, Trans. Am. Soc. Heat. Refrig. Air Cond. Eng. **89**, 500 (1983).

[5] D. Sonntag, Z. Meteorol. **3**, 51 (1994).

[6] W. Wagner and A. Pruß, J. Phys. Chem. Ref. **31**, 387 (2002), doi:10.1063/1.1461829.

[7] L. Buck, J. Appl. Meteorol. **20**, 1527 (1981).

[8] Buck Research Manual (1996).

[9] D. Bolton, Monthly Weather Review **108**, 1046 (1980).

[10] *CIMO Guide*, WMO-No. 8 (2008).

[11] D. M. Murphy, T. Koop, Q. J. Meteorol. Soc. **131**, 1539 (2005), doi:10.1256/qj.04.94.

[12] V. Holten, J. V. Sengers and M. A. Anisimov, J. Phys. Chem. Ref. Data **43**, 043101 (2014).

[13] IAPWS, *Guideline on Thermodynamic Properties of Supercooled Water* (2015), http://www.iapws.org/relguide/Supercooled.pdf.

[14] R. J. Speedy and C. A. Angell, J. Chem. Phys. **65**, 851 (1976).

[15] K. Scheel and W. Heuse, W. Ann. Phys. **29**, 723 (1909).

[16] G. Bottomley, Austr. J. Phys. **31**, 1177 (1978).

[17] G. Kraus and S. Greer, J. Phys. Chem. **88**, 4781 (1984).

[18] N. Fukuta and C. Gramada, J. Atmos. Sci. **60**, 1871 (2003).

[19] G. Beltramino, L. Rosso, D. Smorgon and V. Fernicola, J. Chem. Therm. **105**, 159 (2017).

[20] S. C. Mossop, Proc. Phys. Soc. London Sect. B **68**, 193 (1955).

[21] H. Hanno, R. J. Speedy and C. A. Angell, Science **189**, 880 (1975).

[22] O. Mishima and H. E. Stanley, Nature (London) **396**, 329 (1998), doi: 10.1038/24540.

[23] E. B. Moore and V. Molinero, Nature (London) **479**, 506 (2011), doi: 10.1038/nature10586.

[24] V. Holten, C. E. Bertrand, M. A. Anisimov and J. V. Sengers, J. Chem. Phys. **136**, 094507 (2012), doi: 10.1063/1.3690497.

[25] J. Sellberg et al., Nature (London) **510**, 381 (2014), doi: 10.1038/nature13266.

[26] W. Cantrell, E. Ochshorn, A. Kostinski and K. Bozin, J. Atmos. Oceanic Technol. **25**, 1724 (2008); **26**, 853 (2009), doi:10.1175/2008/JTECHA1028.1.

[27] C. L. Hosler and C. R. Hosler, Trans. Am. Geophys. Union, **36**, Issue 1, 126 (1955), doi: 10.1029/TR036i001p00126

[28] L.A. Guildner, D.P. Johnson and F.E. Jones, J. Res. Natl. Bur. Stand. **80**, 505 (1976), doi:10.6028/jres.080A.054.

[29] T. Takaishi and Y. Sensui, Trans. Faraday Soc. **59**, 2503 (1963).

[30] I. Yasumoto, J. Phys. Chem. **84**, 589 (1980).

[31] IAPWS, *Revised Release on the Pressure along the Melting and Sublimation Curves of Ordinary Water Substance* (2011), http://www.iapws.org.

[32] V. Fernicola, L. Rosso and M. Giovannini, Int. J. Thermophys. **33**, 1363 (2012), doi:10.1007/s10765-011-1128-2.

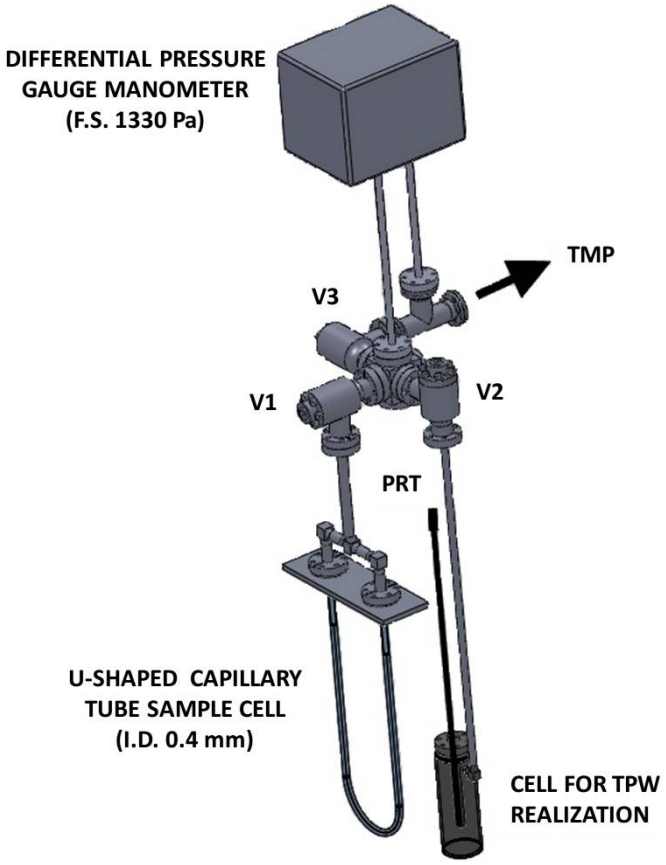

Figure 1. Experimental apparatus for the measurement of saturation water vapour pressure of supercooled water. PRT - platinum resistance thermometer; TPW - triple point of water; TMP - turbo molecular pump; V1-V3 – valve to sample cell, valve to TPW cell and valve to TMP respectively.

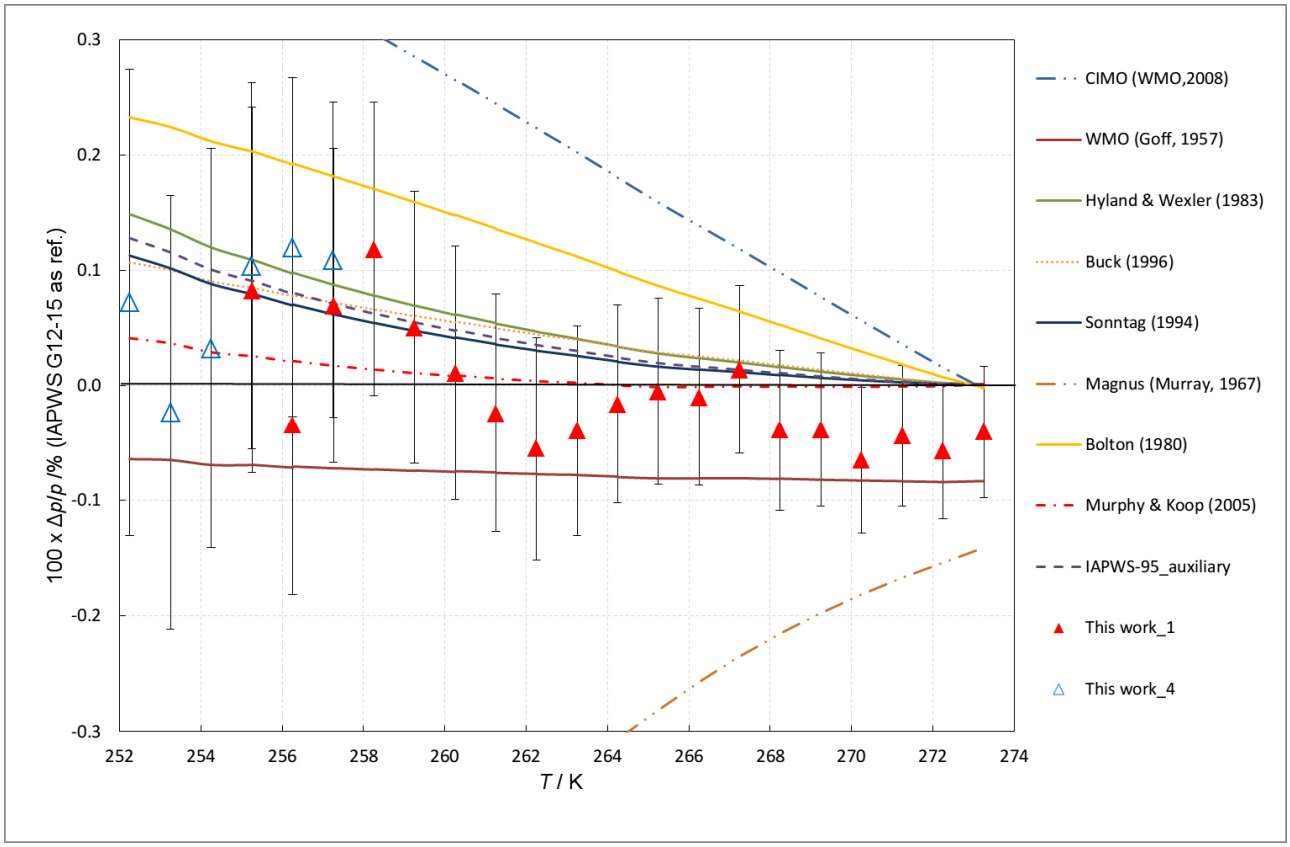

Figure 2. Comparison of the saturation vapour pressure measurements of supercooled water of this work (run 1 and 4) with respect to different formulations. Experimental values are shown with the associated expanded uncertainty (k=2). All data are presented as relative pressure difference, $\Delta p/p$ ×100, using the IAPWS G12-15 formulation as reference, versus the thermodynamic temperature T.

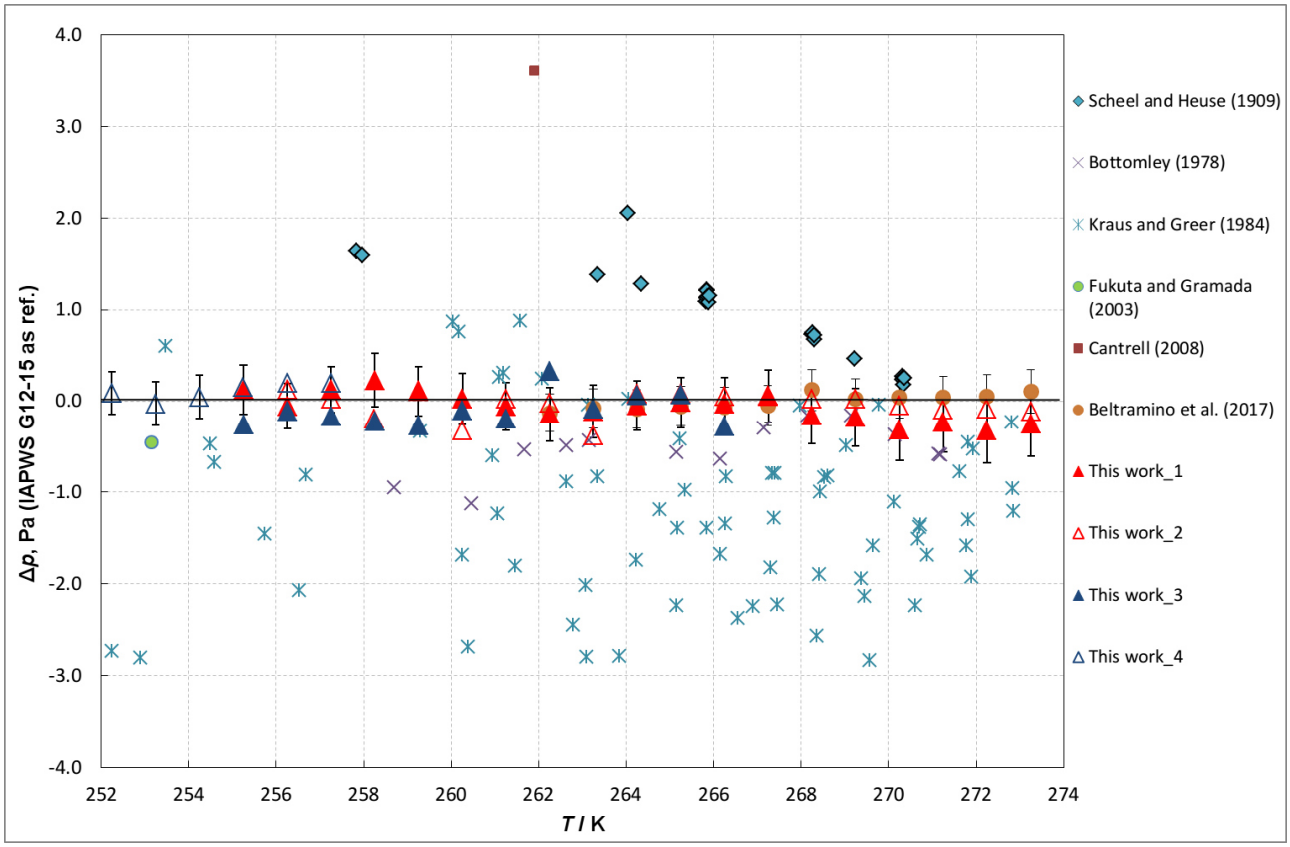

Figure 3. Comparison of the vapour pressure measurements of this work with respect to those available in the literature. Experimental values of this work (run 1 and 4) and of Beltramino *et al.* are shown with the associated expanded uncertainty (k=2). All data are plotted as differences, Δp, with respect to the IAPWS G12-15 equation.

Table I. Percent corrections applied to the raw pressure data. The corrections account for the pressure gauge calibration, the hydrostatic head effect, the thermal transpiration and the adjustment to the measured TPW.

	Percent correction ($100 \times \Delta p/p$)			
T / K	Hydrostatic head	Calibration	Thermal transpiration	Adjustment to TPW
252.248	0.006	-0.728	-0.003	0.013
253.249	0.006	-0.735	-0.003	0.013
254.251	0.006	-0.733	-0.002	0.013
255.251	0.006	-0.732	-0.002	0.013
256.253	0.006	-0.730	-0.002	0.013
257.255	0.006	-0.729	-0.001	0.013
258.248	0.006	-0.721	-0.001	0.013
259.249	0.006	-0.719	-0.001	0.013
260.252	0.006	-0.717	-0.001	0.013
261.248	0.006	-0.714	-0.001	0.013
262.250	0.006	-0.712	-0.001	0.013
263.247	0.006	-0.709	0.000	0.013
264.246	0.006	-0.706	0.000	0.013
265.248	0.006	-0.703	0.000	0.013
266.246	0.006	-0.700	0.000	0.013
267.244	0.006	-0.697	0.000	0.013
268.240	0.006	-0.693	0.000	0.013
269.240	0.006	-0.689	0.000	0.013
270.248	0.006	-0.685	0.000	0.013
271.245	0.006	-0.680	0.000	0.013
272.246	0.006	-0.675	0.000	0.013
273.251	0.006	-0.670	0.000	0.013

Table II. Measured values of saturation vapour pressure, p, of supercooled water and corresponding temperature, T. The combined expanded (k = 2) uncertainty $U_c(p)$ and the relative uncertainty $U_c(p)/p$ are reported. The expanded uncertainty of the temperature $U_c(T)$ is also listed. The uncertainty $U_c(p)$ is obtained from the combination of the standard uncertainty, $u_c(T)$, of temperature measurements (see Table III) and the standard uncertainty, $u_c(p)$, of saturation vapour pressure measurements (see Table IV). Letters from A to D indicate the different measurement runs.

A)

T / K	$U_c(T)$ / K	p / Pa	$U_c(p)$ / mPa	$100\times U_c(p)/p$ / %
255.256	0.006	150.31	240	0.16
256.257	0.006	163.35	243	0.15
257.258	0.006	177.78	245	0.14
258.253	0.006	193.14	248	0.13
259.254	0.006	209.54	251	0.12
260.257	0.006	227.26	254	0.11
261.253	0.006	246.19	258	0.10
262.255	0.006	266.66	263	0.10
263.251	0.006	288.62	269	0.09
264.247	0.006	312.21	274	0.09
265.250	0.006	337.64	281	0.08
266.248	0.006	364.71	288	0.08
267.246	0.006	393.79	296	0.08
268.242	0.006	424.55	305	0.07
269.242	0.006	457.78	315	0.07
270.250	0.006	493.49	326	0.07
271.247	0.006	531.47	338	0.06
272.248	0.006	571.96	351	0.06
273.251	0.006	615.46	360	0.06

B)

T / K	$U_c(T)$ / K	p / Pa	$U_c(p)$ / mPa	$100\times U_c(p)/p$ / %
256.254	0.006	163.49	243	0.15
257.257	0.006	177.67	245	0.14
258.249	0.006	192.66	248	0.13
259.251	0.006	209.50	251	0.12
260.253	0.006	226.85	254	0.11
261.250	0.006	246.22	258	0.10
262.252	0.006	266.73	263	0.10
263.248	0.006	288.29	269	0.09
264.247	0.006	312.34	274	0.09
265.250	0.006	337.74	281	0.08
266.247	0.006	364.77	288	0.08
267.245	0.006	393.77	296	0.08
268.241	0.006	424.70	305	0.07
269.241	0.006	457.96	315	0.07
270.249	0.006	493.72	326	0.07
271.247	0.006	531.60	338	0.06
272.247	0.006	572.16	351	0.06
273.251	0.006	615.60	360	0.06

C)

T / K	$U_c(T)$ / K	p / Pa	$U_c(p)$ / mPa	$100 \times U_c(p)/p$ / %
255.256	0.006	149.93	240	0.16
256.255	0.006	163.26	243	0.15
257.258	0.006	177.49	245	0.14
258.253	0.006	192.69	248	0.13
259.254	0.006	209.16	251	0.12
260.256	0.006	227.13	254	0.11
261.253	0.006	246.06	258	0.10
262.255	0.006	267.13	263	0.10
263.251	0.006	288.65	269	0.09
264.247	0.006	312.31	274	0.09
265.250	0.006	337.73	281	0.08
266.248	0.006	364.47	288	0.08

D)

T / K	$U_c(T)$ / K	p / Pa	$U_c(p)$ / mPa	$100 \times U_c(p)/p$ / %
252.248	0.006	116.12	235	0.20
253.249	0.006	126.50	238	0.19
254.251	0.006	137.93	239	0.17
255.251	0.006	150.28	240	0.16
256.253	0.006	163.55	243	0.15
257.255	0.006	177.81	245	0.14

Table III. Standard uncertainty contributions and combined standard uncertainty, $u_c(T)$, of temperature measurements at 253 K, 263 K and 273 K, to which saturation vapour pressures of about 127 Pa, 289 Pa and 615 Pa correspond.

	T = 253 K (p ≈ 127 Pa)	**T = 263 K (p ≈ 289 Pa)**	**T = 273 K (p ≈ 615 Pa)**
TEMPERATURE MEASUREMENTS	**$u(T)$ / mK**	**$u(T)$ / mK**	**$u(T)$ / mK**
SPRT Calibration	0.2	0.2	0.2
Resistance Bridge Linearity	2.7	2.8	2.9
Meas. Repeatability (incl. Bath Stability)	1.1	1.1	1.1
Bath Temperature Uniformity	0.8	0.8	0.8
Combined Standard Uncertainty, $u_c(T)$	3.0	3.1	3.2

Table IV. Standard uncertainty contributions and combined standard uncertainty, $u_c(p)$, of saturation vapour pressure measurements of 127 Pa, 289 Pa and 615 Pa.

	p ≈ 127 Pa T = 253 K	**p ≈ 289 Pa T = 263 K**	**p ≈ 615 Pa T = 273 K**
PRESSURE MEASUREMENTS	**$u(p)$ /mPa**	**$u(p)$ /mPa**	**$u(p)$ /mPa**
TPW Uncertainty	18.8	18.8	18.8
Manometer calibration	112.3	112.6	113.3
Gage Zero&Span Drift (4 ppm F.S./day)	3.1	3.1	3.1
Extrapolation to time zero	0.4	0.5	0.7
Hydrostatic Head Correction	0.1	0.2	0.3
Thermomolecular Effect Correction	1.4	1.4	1.4
Residual Gases Effect	0.3	0.3	0.3
Combined Standard Uncertainty, $u_c(p)$	113.9	114.2	114.9